atmosphere

MDPI

Article

Analytical Solution for One-Dimensional Gas Pressure Distribution Considering the Variation of Gas Permeability Coefficients with Burial Depth

Jing Yu [1], Haijie He [1,2,3,*], Junding Liu [1,*], Jie Yang [4,*], Ke Xu [4], Guannian Chen [5] and Tao Wu [6]

[1] College of Civil and Architectural Engineering, Taizhou University, Taizhou 318000, China; yujing79@tzc.edu.cn
[2] College of Civil and Architectural Engineering, Zhejiang University, Hangzhou 310058, China
[3] Fangyuan Construction Group Co., Ltd., Taizhou 318000, China
[4] Zhejiang Fang Yuan New Materials Co., Ltd., Taizhou 318000, China; xuk@fyg.cn
[5] School of Civil & Environmental Engineering and Geography Science, Ningbo University, Ningbo 315211, China; chenguannian@nbu.edu.cn
[6] Jiangsu Province Engineering Research Center of Geoenvironmental Disaster Prevention and Remediation, Jiangsu University of Science and Technology, Zhenjiang 212000, China; chinawt@just.edu.cn
* Correspondence: he_haijie@zju.edu.cn (H.H.); junding@tzc.edu.cn (J.L.); zjujack@zju.edu.cn (J.Y.)

Abstract: Landfill gas generated by municipal solid waste (MSW) landfills is the world's third largest source of greenhouse gas emissions. Additionally, the accumulation of landfill gas in waste piles can trigger instability in landfill piles. Based on the exponential distribution pattern of the variation of gas permeability coefficients with burial depth measured in situ, this paper presents an analytical solution for landfill gas-pressure distribution that is more in line with on-site conditions and has been verified by numerical calculations. Compared with cases where the gas permeability coefficient of landfill piles remains constant, the consideration that the gas permeability coefficient of MSW decreases exponentially with increasing burial depth is more likely to cause the accumulation of landfill gas at the landfill bottom, leading to higher gas pressure that can be more than five times higher than that in the former case. Based on a numerical analysis of gas extraction simulations, constant pressure gas extraction is relatively more effective in that a relative pressure of −0.1 kPa can lower the gas pressure in almost the entire pile, while bottom drainage fails to completely collect landfill gas even using a flux of 10–30 times ML.

Keywords: landfill gas; gas permeability coefficient; gas pressure distribution; analytical solution

Citation: Yu, J.; He, H.; Liu, J.; Yang, J.; Xu, K.; Chen, G.; Wu, T. Analytical Solution for One-Dimensional Gas Pressure Distribution Considering the Variation of Gas Permeability Coefficients with Burial Depth. *Atmosphere* **2023**, *14*, 1344. https://doi.org/10.3390/atmos14091344

Academic Editor: Iustinian Gabriel Bejan

Received: 10 May 2023
Revised: 9 August 2023
Accepted: 22 August 2023
Published: 26 August 2023

1. Introduction

Landfill gas is produced by the microbial degradation of municipal solid waste (MSW) [1,2]. It migrates along the path of least resistance and eventually diffuses into the surrounding atmosphere due to the combined effects of concentration and pressure differences [3–7]. The main components of landfill gas are methane (CH_4) and carbon dioxide (CO_2). Methane accounts for approximately 50% of the gas volume and has a greenhouse effect of 21 times that of CO_2. The methane emissions from landfills contribute to 13–20% of total global methane emissions, making it the third largest anthropogenic source of methane emissions after wetlands and rice fields. Uncontrolled emissions of landfill gas can exacerbate global warming, highlighting the importance of the effective management and control of landfill gas emissions [8,9]. Additionally, if landfill gas cannot be effectively drained from the landfill in time, it can accumulate in the pile, which can increase the gas pressure, raise the water level of the leachate inside the pile, and reduce the effective stress of the pile. These factors may lead to the instability and even slippage of the landfill pile [10–15].

Scholars have proposed a one-dimensional finite difference convection–diffusion model for landfill gas to analyze the gas pressure distribution inside landfill piles, which considers the variation patterns of gas pressure and concentration over time [16–20]. Chen et al. [21–24] developed a gas migration model based on the porous media fluid dynamics theory that accounts for the impact of water content changes inside piles on the gas pressure distribution. Townsend et al. [25] proposed a one-dimensional steady-state gas pressure distribution model based on Darcy's law and provided its analytical solution; the model analyzed the effects of the landfill thickness, gas generation rate, and intrinsic permeability coefficient on the gas pressure distribution. Additionally, the study compared the gas collection effects of the leachate drainage layer at the bottom of the landfill and the geomembrane on the top. Ma et al. [26] developed a one-dimensional steady-state gas pressure distribution model that took into account the layered characteristics of the horizontal permeable layer and waste. The model analyzed the effects of the gas generation rate, intrinsic permeability coefficient, intermediate cover layer, high-permeability horizontal permeable layer, and landfill gas drainage channel on the gas pressure distribution. Analytical solutions for the gas migration process through layered MSWs have also been proposed in Zeng [27], Zhang et al. [28], and Wu et al. [29].

However, the gas permeability values used in the aforementioned research works were estimated under the assumption that MSW is a homogeneous material with a constant gas permeability coefficient throughout the landfill. In real-world conditions, the gas permeability coefficient of MSW is influenced by various factors such as its pore structure and water content. The gas permeability coefficient of waste in landfills decreases significantly with depth due to the smaller pores and higher saturation caused by settlement deformation and the downward movement of leachate. This trend is exacerbated by the fact that older waste is typically more compacted at greater depths within the landfill [30,31]. Wei et al. [31] investigated the characteristics of landfill waste composition, density, and water content and conducted experiments to measure the gas permeability coefficient of waste samples obtained from field drilling. They analyzed the effects of porosity, saturation, and waste composition on gas permeability and established the relationship between waste gas permeability and saturation based on the water retention curve of the waste. For a given composition and porosity, the gas permeability coefficient of the waste increased exponentially with increasing porosity. Furthermore, for a given porosity, the gas permeability of the waste at low saturation was higher than that at high saturation, and this difference increased with increasing porosity. Moreover, under the same porosity and saturation, the gas permeability coefficient of the waste in specimens increased with increasing landfill age. To estimate the gas permeability coefficient in a landfill, Jain et al. [30] injected air into three vertical wells at different depths. The results showed that the measured gas permeability of waste decreased significantly with increasing depth, ranging from 3.2×10^{-11} to 1.6×10^{-13} m^2. This decrease was mainly attributed to the larger overburden pressure that reduced the porosity of the MSW.

In conclusion, the decreases in the gas permeability coefficient with increasing burial depth need to be taken into consideration when analyzing the gas pressure distribution in waste piles. This paper proposes an analytical model for the gas pressure distribution that incorporates the actual variation in gas permeability coefficients with burial depth, which is validated through finite element calculations. The analysis of gas pressure distribution patterns at impermeable boundaries and at the landfill bottom with gas extraction and drainage is possible with the proposed solution. This paper also investigates the effects of the gas generation rate, pile thickness, gas permeability coefficient, and gas extraction pressure/rate on the gas pressure inside the pile, providing a foundation and guidance for the assessment of landfill gas collection and subsequent stability analyses of the pile in terms of landfill gas pressure.

2. Theoretical Model

2.1. Derivation of Analytical Solutions

Assuming that the migration rate of water in the waste is much lower than that of the landfill gas, and that the action time of leachate is very long, the migration of leachate can be ignored when simulating gas migration. To establish the gas migration control equation in the waste, the following assumptions were made, as seen in Figure 1:

(1) The migration of landfill gas was treated as the migration of a single mixed gas;
(2) The gas generation rate inside the landfill reached a steady state, and the gas generation rate in a certain period was constant;
(3) The migration of landfill gas in the waste followed Darcy's law;
(4) The waste was an isothermal homogeneous body.

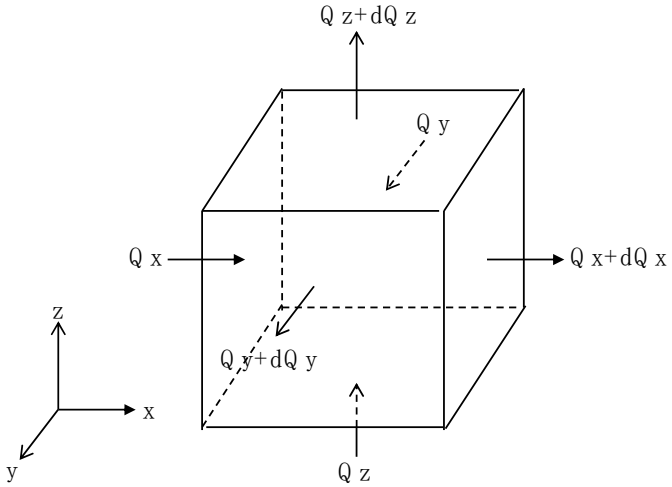

Figure 1. A schematic of a gas migration unit in a landfill.

The mass conservation equation for porous media fluids is:

$$\frac{\partial}{\partial t}(\rho_g \theta_g) + \nabla \cdot (\rho_g v_g) = Q_g \tag{1}$$

where ρ_g is the density of landfill gas in kg/m^3, θ_g is the landfill gas volume fraction, v_g is the landfill gas migration rate in m/s, and Q_g is the gas generation rate in kg/(m^3·s). To simplify the calculation, the landfill was simplified as a one-dimensional model, and according to Darcy's law:

$$v_g = -\frac{k_g}{\mu}\frac{\partial P}{\partial z} \tag{2}$$

where μ is the landfill gas viscosity coefficient in Pa·s and k_g is the intrinsic gas permeability coefficient of the waste soil in m^2. The following exponential function was used in this paper to characterize its relationship with burial depth:

$$k_g = \beta e^{-\alpha z} \tag{3}$$

Based on actual measurements of gas permeability coefficients at different depths from the research of Wei et al. [31] and Jain et al. [30], the values of α and β were approximated as 0.22 (m^{-1}) and 2.26 × 10^{-11} (m^2), respectively. These values were calculated with the surface serving as the coordinate origin and are shown in Figure 2.

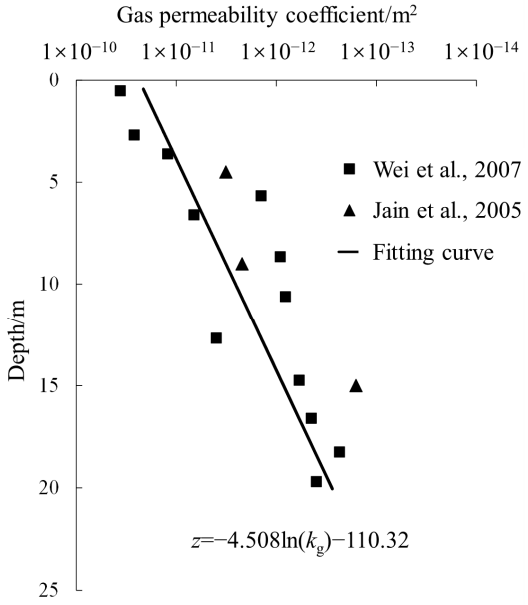

Figure 2. Variation pattern of gas permeability coefficient with burial depth [30,31].

According to the ideal gas equation of state, the landfill gas density can be written as an expression for the pressure P:

$$P = \frac{m}{V}\frac{1}{M}RT = \frac{\rho_g}{M}RT \tag{4}$$

where V is the volume of landfill gas in m^3, m is the mass of landfill gas in kg, M is the average molar mass of landfill gas in g/mol, R is the ideal gas constant in 8.314 J/(mol·K), and T is the temperature of the system in K. For the one-dimensional steady-state problem under consideration, taking Equation (4) into Equations (1)–(3) yields:

$$\frac{M}{\mu RT}\frac{\partial}{\partial z}\left(-k_g P\frac{\partial P}{\partial z}\right) = Q_g \tag{5}$$

That is,

$$-\frac{\alpha\beta M}{2\mu RT}e^{-\alpha z}\frac{\partial(P^2)}{\partial z} + \frac{\beta M}{2\mu RT}e^{-\alpha z}\frac{\partial^2(P^2)}{\partial z^2} + Q_g = 0 \tag{6}$$

Let

$$A = -\frac{2Q_g\mu RT}{\beta M} \tag{7}$$

Then,

$$Ae^{\alpha z} = -\alpha\frac{\partial(P^2)}{\partial z} + \frac{\partial^2(P^2)}{\partial z^2} \tag{8}$$

To facilitate subsequent calculations, the general solution of Equation (8) can be written as:

$$\frac{\partial(P^2)}{\partial z} = Aze^{\alpha z} + (\alpha C_1 + 1\frac{A}{\alpha})e^{\alpha z} \tag{9}$$

Further integration of Equation (9) yields:

$$P = \sqrt{\frac{A}{\alpha}ze^{\alpha z} + C_1e^{\alpha z} + C_2} \tag{10}$$

where C_1 and C_2 are constants to be determined. When the upper and lower boundaries of the landfill are constant pressure boundaries (i.e., Dirichlet boundary conditions), assuming

that the gas pressure values at the upper and lower boundaries (at z_u and z_l) are P_u and P_l, respectively, then:

$$P_u^2 = \frac{A}{\alpha} z_u e^{\alpha z_u} + C_1 e^{\alpha z_u} + C_2 \tag{11}$$

$$P_l^2 = \frac{A}{\alpha} z_l e^{\alpha z_l} + C_1 e^{\alpha z_l} + C_2 \tag{12}$$

Solving Equations (11) and (12) yields:

$$C_1 = \frac{P_u^2 - P_l^2 - \frac{A}{\alpha}(z_u e^{\alpha z_u} - z_l e^{\alpha z_l})}{e^{\alpha z_u} - e^{\alpha z_l}} \tag{13}$$

$$C_2 = \frac{e^{\alpha z_u} P_l^2 - e^{\alpha z_l} P_u^2 + \frac{A}{\alpha} e^{\alpha (z_u + z_l)} (z_u - z_l)}{e^{\alpha z_u} - e^{\alpha z_l}} \tag{14}$$

Under the gas drainage condition at the landfill bottom, it can be considered that the upper boundary of the landfill is still a constant pressure boundary $P_u(z_u)$. At this time, the lower boundary at z_l is a constant flux boundary with a flux value of ω_l. For any location, the flux per unit area inside the landfill is:

$$\omega = \rho_g v_g = -\frac{PM}{\mu RT} k_g \frac{\partial P}{\partial z} = -\frac{\beta M}{2\mu RT} e^{-\alpha z} \frac{\partial (P^2)}{\partial z} = Q_g (z + \frac{\alpha}{A} C_1 \frac{1}{\alpha}) \tag{15}$$

Bringing in the lower boundary coordinates and associating it with the upper boundary condition equation (Equation (11)), we can solve the constants in Equation (10) as:

$$C_1 = \frac{A}{\alpha} (\frac{\omega_l}{Q_g} - z_l - \frac{1}{\alpha}) \tag{16}$$

$$C_2 = P_u^2 + (z_l - z_u + \frac{1}{\alpha} - \frac{\omega_l}{Q_g}) \frac{A}{\alpha} e^{\alpha z_u} \tag{17}$$

2.2. Model Validation

To validate the accuracy of the proposed analytical solution, the finite element numerical calculation software Comsol was used to compare and verify an example. An extremely fine predefined mesh size was applied in the numerical model, with the configuration of meshes containing 100 elements and the relative tolerance set as 0.001 [32–34]. The boundary conditions of the case included a combination of a constant pressure boundary at the upper boundary and a constant flux boundary at the lower boundary. The analytical solution was then calculated using Equations (10), (16) and (17).

The specific parameters of the example were set as follows: the upper boundary of the landfill was directly connected to the atmospheric pressure, i.e., $P_u - P_0 = 0$, where P_0 was the standard atmospheric pressure of 101.3 kPa; the lower boundary was the impermeable boundary, i.e., the lower boundary flux value $\omega_l = 0$. The molar mass of gas M was 0.03 kg/mol, the dynamic viscosity μ was 1.37×10^{-5} kg/(m·s); the temperature of the landfill T was 298 K (i.e., 25 degrees Celsius), and the gas generation rate Q_g was 4.4×10^{-7} kg/(m^3·s). The calculated steady-state gas pressure distributions for three groups of landfill heights (10, 20, and 30 m) are illustrated in Figure 3. After comparing the results obtained from analytical solutions and the Comsol numerical calculations under the same working conditions, it was observed that the two sets of data were in complete agreement, with all correlation indices over 0.99. This comparison confirms the accuracy of the analytical solutions.

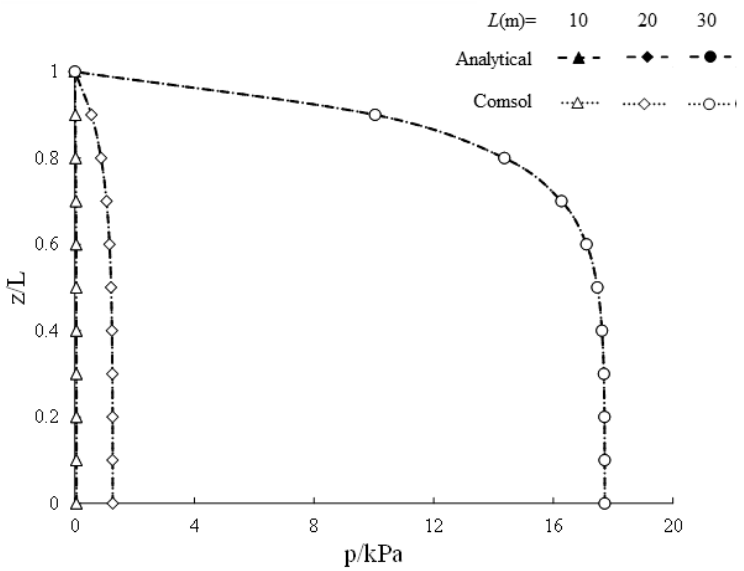

Figure 3. Comparison of analytical solutions and numerical results.

3. One-Dimensional Steady-State Gas Pressure Distribution Pattern

3.1. Gas Pressure Distribution Pattern of Landfill Piles without Gas Drainage

Firstly, the analysis of the gas pressure distribution of landfill piles with an impermeable bottom was conducted, and the parameters used in the model calculation were the same as those used in the previous example—illustrated as dashed lines in Figure 4. For comparison, the results of the one-dimensional steady-state gas pressure distribution without consideration of the variation of gas permeability coefficients with burial depth are also plotted as solid lines in Figure 4, according to the analytical solutions proposed by Townsend et al. [25]. Under this working condition, the bottom of the landfill pile was impermeable, and the generated landfill gas migrated to the top, and finally escaped to the atmosphere. The gas pressure on the top was the atmospheric pressure, and the landfill gas pressure increased as burial depth increased, with the landfill gas pressure at the pile bottom being the largest.

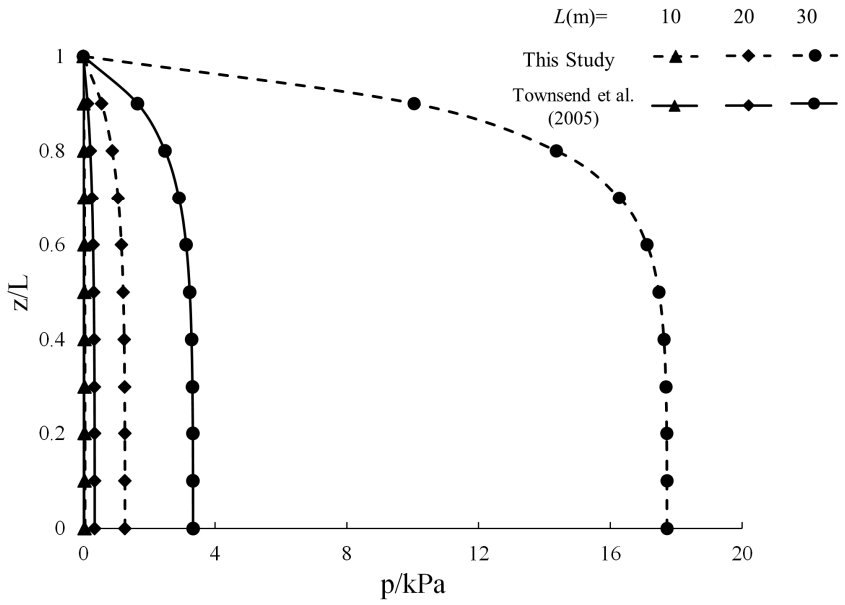

Figure 4. Gas pressure distribution of piles without gas drainage at the bottom [25].

Without considering the variation of gas permeability coefficients with burial depth, the maximum gas pressure reached 0.35 kPa at the bottom within a depth range of 20 m when the thickness was 20 m, and 3.3 kPa at the bottom within a depth range of 30 m when the thickness was 30 m. Under the condition of considering the variation of gas permeability coefficients with burial depth, the landfill gas pressure also increased with increases in burial depth. Under the same pile thickness, when the burial depths were identical, the gas pressure values that took into account the variation of gas permeability coefficients with burial depth were found to be greater than those that did not consider it. It can be concluded that the gas pressure calculated by the proposed method is up to five-times higher than the existing solution proposed by Townsend et al. [25], illustrating a serious accumulation of landfill gas by the relatively low permeability of the pile at a high burial depth.

When the pile thickness was 10 m, the relative pressure values of the gas pressure—considering the variation of gas permeability coefficients with burial depth—were 0.028, 0.043, 0.050, 0.053, and 0.053 kPa at the burial depths of 2, 4, 6, 8, and 10 m, respectively. In contrast, the pressure values of the gas pressure when not considering the variation of gas permeability coefficients with burial depth were 0.012, 0.019, 0.023, 0.026, and 0.026 kPa at the burial depths of 2, 4, 6, 8, and 10 m, respectively. The former was 2.3 times, 2.2 times, 2.2 times, 2.0 times and 2.0 times that the latter when the burial depth of both was identical, under a pile thickness of 10 m. Moreover, as the pile thickness increased, the increase rate of the gas pressure value when considering the variation of gas permeability coefficients with burial depth was greater than that without consideration of the variation of gas permeability coefficients with burial depth.

When the pile thickness was 30 m, the values of the gas pressure when considering the variation of gas permeability coefficients with burial depth were 14.4, 17.1, 17.6, 17.7, and 17.7 kPa at the burial depths of 6, 12, 18, 24, and 30 m, respectively. In contrast, the values of the gas pressure when not considering the variation of gas permeability coefficients with burial depth were 2.5, 3.1, 3.3, 3.3, and 3.3 kPa at the burial depths of 6, 12, 18, 24, and 30 m, respectively. The former was 5.8 times, 5.5 times, 5.3 times, 5.4 times, and 5.4 times that of the latter when the burial depth of both was identical, under a pile thickness of 30 m—which was significantly higher than the multiplicity observed under the 10 m-thick working condition.

The main reason for this phenomenon is that the permeability coefficient at the bottom is affected by the upper waste pile load, and the gas permeability coefficient becomes smaller as the lower porosity is reduced, blocking the migration of the generated landfill gas to the atmosphere and making it more likely for the landfill gas to accumulate inside the pile. Thus, it needs to accumulate a higher relative gas pressure to vent the same landfill gas production under the same working conditions when considering the variation of gas permeability coefficients with burial depth.

3.2. Gas Pressure Distribution Pattern of Landfill Piles with Gas Extraction and Drainage

Using the 20 m-thick waste pile model as the prototype, the impermeable lower boundary was subjected to a gas extraction condition with an extraction flux of ML ($\omega_l = Q_g L$; the gas extraction rate is equal to the gas generation rate inside the pile). Moreover, the effects of the gas extraction rate, gas generation rate inside the pile, pile thickness, and gas permeability coefficient on the gas pressure distribution inside the waste pile using gas extraction at the bottom were analyzed respectively, as presented in Figure 5.

The landfill gas pressure distribution when extracting gas at the pile bottom for different extraction fluxes is provided in Figure 5a. Compared with the impermeable lower boundary, the landfill gas pressure when extracting with ML was relatively small, but the decrease was insignificant and the gas pressure inside the pile was under positive pressure. The pressure values at the burial depths of 4, 8, 12, 16, and 20 m were 0.86, 1.13, 1.20, 1.19, and 1.18 kPa when the extraction flux was ML, which were 98%, 97%, 97%, 94%, and 93% of those without extraction, respectively. Considering that the gas permeability coefficient

varied with burial depth, the gas generation rate of the entire landfill was used as the bottom landfill gas collection rate, and most of the landfill gas failed to be collected by the collection system.

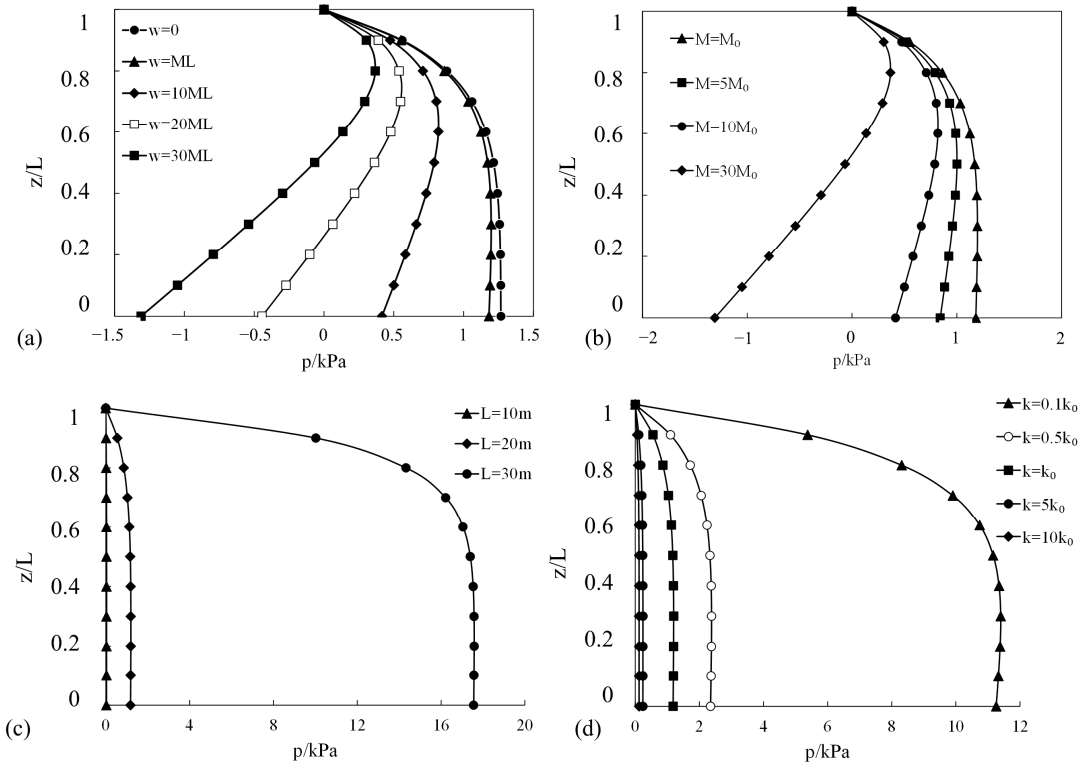

Figure 5. Landfill gas pressure distribution at the bottom flux boundary. (**a**) Gas extraction pressure. (**b**) Gas generation rate. (**c**) Pile thickness. (**d**) Gas permeability coefficient.

When 10 times the entire generation rate was used as the bottom landfill gas collection rate, although the gas pressure values at different burial depths inside the landfill piles were smaller than when no gas was extracted, they were still higher than the atmospheric pressure at all places in the pile. When 20 times the entire generation rate was used as the bottom landfill gas collection rate, the 6 m range at the bottom was under negative pressure and the landfill gas in this range was effectively collected, while the landfill gas in the upper 14 m range failed to be effectively collected. Even using 30 times the entire generation rate as the bottom landfill gas collection rate, the landfill gas in the upper 8 m range failed to be effectively collected. The variation of gas permeability coefficients with burial depth obviously influenced the collection efficiency of the landfill gas, and the bottom gas collection method was unsuitable for landfill gas collection.

Figure 5b shows the gas pressure distribution inside the pile when the extraction flux of ML was used at the bottom for different waste gas generation rates. When the gas generation rate of the landfill gas was 4.4×10^{-7} kg/(m^3·s) and the bottom was extracted with the ML flux, the landfill gas in the entire field failed to be effectively collected and the pressure values were positive everywhere; when the gas generation rate of the landfill gas was 1.32×10^{-5} kg/(m^3·s) and the bottom was extracted with the ML flux, the landfill gas in most parts of the pile could be effectively collected, and the landfill gas pressure within this range was all negative.

Figure 5c presents the gas pressure distribution inside the pile when the extraction flux of ML was used at the bottom for different waste pile thicknesses. When the pile thickness was 10 m, the gas permeability coefficient of the pile was relatively large, and the landfill gas inside the pile could be effectively collected when the negative pressure extraction was performed at the bottom. All parts of the pile were in the negative pressure extraction state,

and the average gas pressure value within the depth range of 10 m was −0.06 kPa, while the landfill gas pressure at the pile bottom was −0.16 kPa.

The results indicate that when the pile thickness was 10 m, the flux used at the bottom satisfied the landfill gas collection requirements. When the pile thickness was 30 m, the gas permeability coefficient of the middle and lower parts of the pile was small, and the landfill gas inside the pile could not be effectively collected when extracting gas at the bottom, and the maximum pressure of the landfill gas reached 16.6 kPa. When the pile thickness was 30 m, the landfill gas pressure at the upper part of the pile increased rapidly, from 0 kPa at the ground level to 9.8 kPa at 3 m, then to 14.0 kPa at 6 m and 15.7 kPa at 9 m. When it rose to 15 m, the pressure value reached a maximum of 16.6 kPa. The pressure values all over the bottom were affected by the collection system and tended to decrease at a low rate. The pressure at the depth of 30 m reached 16.1 kPa, which was 3% lower than the maximum gas pressure.

Figure 5d illustrates the gas pressure distribution inside the pile when the extraction flux of ML was used at the depth of 20 m for different gas permeability coefficients. When measures were taken to change the permeability coefficient of the pile, the gas pressure values inside the pile changed significantly. The shapes of the landfill gas pressure curves under different permeability coefficients were similar—all indicating that the pressure growth of landfill gas was mainly concentrated in the middle and upper parts of the pile, while it can be seen that decrease/increases in the pile gas pressure compared with the prototype were almost the same as the increase/decreases in the permeability coefficient. The increase in the permeability coefficient made the landfill gas collection efficiency significantly optimized, and conversely, the smaller permeability coefficient further increased the gas pressure inside the pile, which is less favorable for gas drainage.

3.3. Gas Pressure Distribution Pattern of Landfill Piles with Constant Pressure Gas Extraction

The example model of a 20 m-thick waste pile was used as the prototype, and the impermeable lower boundary was subjected to a constant negative pressure (−1 kPa relative pressure as the reference model) for the gas extraction condition. The effects of the gas extraction rate, gas generation rate inside the pile, pile thickness, and gas permeability coefficient on the gas pressure distribution inside the waste pile using gas extraction at the bottom were analyzed, respectively, as displayed in Figure 6.

The gas pressure distribution inside the pile under different extraction pressures is shown in Figure 6a. When the gas extraction ended and the pile reached a stable state, the landfill gas pressure reached 0.66 kPa at 2.5 m below the ground and exceeded 1 kPa from 5 m below the ground to the bottom of the pile. When the negative-pressure 0.1 kPa landfill gas collection pipe was arranged at the pile bottom, it significantly reduced the landfill gas pressure inside the pile. The gas pressure within the range from the top to 17.5 m below the ground exceeded the atmospheric pressure, but the relative pressure values decreased significantly compared with those without gas extraction—with the decrease ranging from 95% to 98%, respectively. When a negative pressure of −0.1 kPa was used for the landfill gas collection, the pressure values were close to 0 kPa at all places in the pile, and the negative pressure of 0.1 kPa extraction met the landfill gas collection requirements under this working condition. When the negative pressure rose to 1 kPa, the negative pressure transfer effect became more and more obvious, and the average relative pressure value within the range of 7.5 m at the bottom reached −0.95 kPa.

Figure 6b shows the gas pressure distribution inside the 20 m-thick pile when −1 kPa was used at the bottom for different waste gas generation rates. With increases in the waste gas generation rate, the pressure required for landfill gas collection increased. When the landfill gas generation rate was 4.4×10^{-7} kg/(m^3·s), the landfill gas in the entire field was effectively collected under −1 kPa, and the pressure values were negative at all places in the pile; when the landfill gas generation rate was 4.4×10^{-6} kg/(m^3·s), the landfill gas in the upper 10 m of the pile failed to be completely collected under the working pressure of −1 kPa, and the pressure value at 2.5 m below the ground level reached a maximum

of 0.68 kPa. Therefore, when a landfill adopts biorecharge technology to enhance the gas generation rate of waste, it is necessary to increase the landfill gas collection pressure at the bottom.

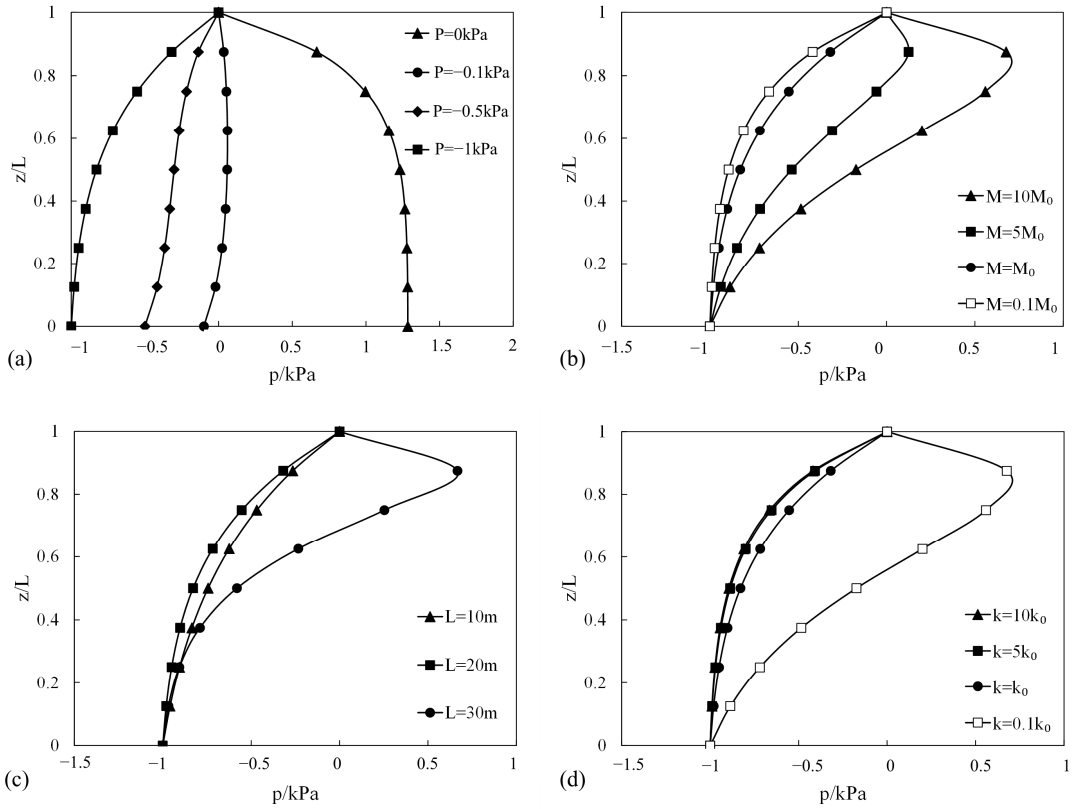

Figure 6. Landfill gas pressure distribution at the bottom pressure boundary. (**a**) Gas extraction pressure. (**b**) Gas generation rate. (**c**) Pile thickness. (**d**) Gas permeability coefficient.

Figure 6c illustrates the gas pressure distribution inside the pile when −1 kPa was used at the bottom for different pile thicknesses. The landfill gas in the 10 m- and 20 m-thick piles was effectively collected, and the gas pressure values at all places in the pile were less than those at atmospheric pressure. At this time, the negative pressure was transferred to the upper part of the pile through the pores of the waste, and the negative pressure showed a trend of gradually decreasing from the bottom to the top. Meanwhile, the landfill gas in the 30 m-thick pile had a nearly 9 m positive pressure area, which was concentrated in the upper region of the pile, resulting in the overflow of landfill gas generated in the upper part of the pile from the upper interface. The main reason for this phenomenon is that the bottom of the 30 m-thick pile was subjected to large loads, small pores, and small permeability coefficients; the pile was thicker and the negative pressure at the bottom was attenuated significantly in the process of transference to the top waste.

Figure 6d displays the gas pressure distribution inside the 20-m thick pile when −1 kPa was used at the bottom for different gas permeability coefficients. The landfill gas pressure is inversely proportional to the gas permeability coefficient of waste, and the smaller the permeability coefficient, the higher the landfill gas pressure. Under the conditions of increasing the permeability coefficient, the landfill gas was effectively collected under −1 kPa at the bottom, and the gas pressure values at all places in the pile were less than those at atmospheric pressure; while under the condition of decreasing the permeability coefficient by 10 times compared with the prototype, the landfill gas inside the pile with a thickness of nearly 10 m failed to be effectively collected and was concentrated in the middle and upper regions of the pile.

4. Conclusions

Based on the exponential distribution pattern of the variation of gas permeability coefficients with burial depth measured in situ, this paper presents an analytical solution for landfill gas pressure distribution that is more in line with on-site conditions that has been verified by numerical calculations. Through numerical analysis, the following conclusions were obtained:

- The accumulation of landfill gas at the landfill bottom is relatively more likely when the gas permeability coefficient of MSW decreases exponentially with increasing burial depth, leading to higher gas pressure that can be more than five-times higher than that in a constant permeability case.
- Using the bottom drainage technique with a flux of 10–30 times ML fails to completely collect landfill gas. Therefore, bottom drainage is unsuitable for situations where the on-site gas permeability coefficient decreases with increasing burial depth.
- Constant pressure gas extraction at a relative pressure of −0.1 kPa can reduce the gas pressure in almost the entire pile to a value lower than the atmospheric pressure, and the extraction effect is significantly improved with further reductions in extraction pressure. Constant pressure gas extraction is more suitable for on-site waste piles.
- Increases in pile height, the acceleration of the gas generation rate, and decreases in the basic permeability coefficient are all detrimental to gas extraction and drainage efficiency. The gas extraction rate or pressure should be determined according to the actual parameters of the waste pile to ensure optimal efficiency.
- In future research, transient simulations of landfill gas extraction considering decreasing permeability with burial depth is to be conducted, simulating the gas accumulating process at the early stage of MSWs, as well as the gas extraction rate needed for attenuating gas-generating scenarios—e.g., MSWs already worked for decades.

Author Contributions: Conceptualization, H.H. and T.W.; Methodology, H.H., J.Y. (Jing Yu) and G.C.; Validation, H.H. and T.W.; Formal Analysis, H.H. and J.L.; Investigation, K.X.; Resources, H.H. and J.Y. (Jie Yang); Writing—Original Draft Preparation, J.Y. (Jing Yu) and H.H.; Writing—Review & Editing, J.Y. (Jie Yang), J.Y. (Jing Yu) and J.L.; Supervision, G.C. and K.X.; Project Administration, H.H. and K.X.; Funding Acquisition, H.H. All authors have read and agreed to the published version of the manuscript.

Funding: This research was funded by the Natural Science Foundation of Zhejiang Province (LQ21E080003), "Pioneer" and "Leading Goose" R&D Program of Zhejiang (2022C03051, 2023C04033), Science and technology project of the Ministry of Housing and Urban-Rural Development (2020-K-026, 2021-K-125), Taizhou science and technology project (22gyb07), and Science and technology project of the Department of housing and urban–rural development of Zhejiang Province (2020-K-164).

Institutional Review Board Statement: Not applicable.

Informed Consent Statement: Not applicable.

Data Availability Statement: The data that support the findings of this study are available from the corresponding author upon reasonable request.

Conflicts of Interest: The authors declare that they have no conflict of interest regarding the publication of this paper.

References

1. Borisova, D.; Kostadinova, G.; Petkov, G.; Dospatliev, L.; Ivanova, M.; Dermendzhieva, D.; Beev, G. Assessment of CH_4 and CO_2 Emissions from a Gas Collection System of a Regional Non-Hazardous Waste Landfill, Harmanli, Bulgaria, Using the Interrupted Time Series ARMA Model. *Atmosphere* **2023**, *14*, 1089. [CrossRef]
2. Xia, T.; Borjigin, S.G.; Raneses, J.; Stroud, C.A.; Batterman, S.A. Mobile Measurements of Atmospheric Methane at Eight Large Landfills: An Assessment of Temporal and Spatial Variability. *Atmosphere* **2023**, *14*, 906. [CrossRef]
3. Chen, Z.; Gong, H.; Zhang, M.; Wu, W.; Liu, Y.; Feng, J. Impact of using high-density polyethylene geomembrane layer as landfill intermediate cover on landfill gas extraction. *Waste Manag.* **2011**, *31*, 1059–1064. [CrossRef]

4. Lei, L.; Bing, L.; Qiang, X.; Ying, Z.; Chun, Y. The modelling of biochemical-thermal coupling effect on gas generation and transport in MSW landfill. *Int. J. Environ. Pollut.* **2011**, *46*, 216–233. [CrossRef]
5. Li, H.; Qin, S.J.; Tsotsis, T.T.; Sahimi, M. Computer simulation of gas generation and transport in landfills: VI-Dynamic updating of the model using the ensemble Kalman filter. *Chem. Eng. Sci.* **2012**, *74*, 69–78. [CrossRef]
6. Xue, Q.; Liu, L. Study on Optimizing Evaluation and Recovery Efficiency for Landfill Gas Energy Collection. *Environ. Prog. Sustain. Energy* **2014**, *33*, 972–977. [CrossRef]
7. He, H.; Wu, T.; Qiu, Z.; Zhao, C.; Wang, S.; Yao, J.; Hong, J. Enhanced Methane Oxidation Potential of Landfill Cover Soil Modified with Aged Refuse. *Atmosphere* **2022**, *13*, 802. [CrossRef]
8. National Academies of Sciences, Engineering, and Medicine. *Negative Emissions Technologies and Reliable Sequestration: A Research Agenda*; The National Academies Press: Washington, DC, USA, 2019.
9. Krzywanski, J.; Ashraf, W.M.; Czakiert, T.; Sosnowski, M.; Grabowska, K.; Zylka, A.; Kulakowska, A.; Skrobek, D.; Mistal, S.; Gao, Y. CO_2 Capture by Virgin Ivy Plants Growing Up on the External Covers of Houses as a Rapid Complementary Route to Achieve Global GHG Reduction Targets. *Energies* **2022**, *15*, 1683. [CrossRef]
10. Sanchez, R.; Tsotsis, T.T.; Sahimi, M. Computer simulation of gas generation and transport in landfills. III: Development of lanfills' optimal model. *Chem. Eng. Sci.* **2007**, *62*, 6378–6390. [CrossRef]
11. Stoltz, G.; Gourc, J.; Oxarango, L. Liquid and gas permeabilities of unsaturated municipal solid waste under compression. *J. Contam. Hydrol.* **2010**, *118*, 27–42. [CrossRef]
12. Garg, A.; Achari, G. A Comprehensive Numerical Model Simulating Gas, Heat, and Moisture Transport in Sanitary Landfills and Methane Oxidation in Final Covers. *Environ. Model. Assess.* **2010**, *15*, 397–410. [CrossRef]
13. Tariku, F.; Kumaran, K.; Fazio, P. Transient model for coupled heat, air and moisture transfer through multilayered porous media. *Int. J. Heat Mass Transf.* **2010**, *53*, 3035–3044. [CrossRef]
14. Li, H.; Sanchez, R.; Qin, S.J.; Kavak, H.I.; Webster, I.A.; Tsotsis, T.T.; Sahimi, M. Computer simulation of gas generation and transport in landfills. V: Use of artificial neural network and the genetic algorithm for short- and long-term forecasting and planning. *Chem. Eng. Sci.* **2011**, *66*, 2646–2659. [CrossRef]
15. Jung, Y.; Imhoff, P.; Finsterle, S. Estimation of Landfill Gas Generation Rate and Gas Permeability Field of Refuse Using Inverse Modeling. *Transp. Porous Media* **2011**, *90*, 41–58. [CrossRef]
16. Findikakis, A.N.; Leckie, J.O. Numerical-simulation of gas-flow in sanitary landfills. *J. Environ. Eng. Div.-ASCE* **1979**, *105*, 927–945. [CrossRef]
17. ElFadel, M.; Findikakis, A.N.; Leckie, J.O. Migration and atmospheric emission of landfill gas. *Hazard. Waste Hazard. Mater.* **1995**, *12*, 309–327. [CrossRef]
18. ElFadel, M.; Findikakis, A.N.; Leckie, J.O. Numerical modelling of generation and transport of gas and heat in landfills 1. Model formulation. *Waste Manag. Res.* **1996**, *14*, 483–504. [CrossRef]
19. ElFadel, M.; Findikakis, A.N.; Leckie, J.O. Numerical modelling of generation and transport of gas and heat in sanitary landfills 2. Model application. *Waste Manag. Res.* **1996**, *14*, 537–551. [CrossRef]
20. ElFadel, M.; Findikakis, A.N.; Leckie, J.O. Gas simulation models for solid waste landfills. *Crit. Rev. Environ. Sci. Technol.* **1997**, *27*, 237–283. [CrossRef]
21. Chen, J.J.; Wang, H.Q.; Wang, J.S. Numerical Model of Landfill Gas Migration. *Environ. Sci.* **1999**, *5*, 96–99. (In Chinese)
22. Chen, J.J.; Wang, H.Q.; Wang, J.S.; Nie, Y.F.; Li, G.D. Numerical Model of Landfill Gas Migration and its Application. *Acta Sci. Circumstantiae* **2000**, *3*, 327–331. (In Chinese)
23. Chen, J.J.; Peng, S.; Wang, J.S. Experimental Study on Parameters Identification for Two-Phase Flow (Water-Air) in Unsaturated Zone. *Adv. Water Sci.* **2001**, *12*, 467–472. (In Chinese)
24. Chen, J.J.; Xie, J.B. Application of boundary element method in numerical modeling of landfill gas migration. *Acta Sci. Circumstantiae* **2008**, *10*, 2141–2147. (In Chinese)
25. Townsend, T.G.; Wise, W.R.; Jain, P. One-dimensional gas flow model for horizontal gas collection systems at municipal solid waste landfills. *J. Environ. Eng.-ASCE* **2005**, *131*, 1716–1723. [CrossRef]
26. Ma, X.F.; Li, Y.C.; Zhan, L.T.; Chen, Y.M. One-dimensional Steady-state Model for Gas Pressure Distribution in Municipal Solid Waste Landfill. *J. Civil. Archi. Environ. Eng.* **2013**, *5*, 8. (In Chinese)
27. Zeng, G. Study on landfill gas migration in landfilled municipal solid waste based on gas-solid coupling model. *Environ. Prog. Sustain* **2020**, *39*, 13352. [CrossRef]
28. Zhang, T.; Shi, J.; Wu, X.; Lin, H.; Li, X. Simulation of gas transport in a landfill with layered new and old municipal solid waste. *Sci. Rep* **2021**, *11*, 9436. [CrossRef]
29. Wu, X.; Shi, J.; Zhang, T.; Li, Y.; Shu, S. Transient and Quasi-Steady-State Analytical Methods for Simulating a Vertical Gas Flow in a Landfill with Layered Municipal Solid Waste. *Mathematics* **2022**, *10*, 3658. [CrossRef]
30. Jain, P. Air permeability of waste in a municipal solid waste landfill. *J. Environ. Eng.-ASCE* **2005**, *131*, 1565–1573. [CrossRef]
31. Wei, H.Y. *Experimental and Numerical Study on Gas Migration in Landfill of Municipal Solid Waste*; Zhejiang University: Hangzhou, China, 2007. (In Chinese)
32. Chen, G.-N.; Li, Y.-C.; Zuo, X.-R.; Ke, H.; Chen, Y.-M. Comparison of adsorption behaviors of Kaolin from column and batch tests: Concept of dual-porosity. *J. Environ. Eng.-ASCE* **2020**, *146*, 04020102. [CrossRef]

33. Chen, G.-N.; Wang, Y.; Wu, T.; Tong, S.; Li, Y.-C.; Ke, H. Single region substitute models for dual-porosity advection-dispersion migration process based on contaminant distribution. *Comput. Geotech.* **2022**, *150*, 104929. [CrossRef]
34. Chen, G.-N.; Li, Y.-C.; Sample-Lord, K.M.; Shan, T. Analytical evaluation of steady-state solute distribution in through-diffusion and membrane behavior test under non-perfectly flushing boundary conditions. *J. Rock Mech. Geotech. Eng.* 2023, *in press*. [CrossRef]